Nucleic Acids Research, 1999, Vol. 27, No. 7 **1619–1624**

DNA minor groove recognition by *bis*-benzimidazole analogues of Hoechst 33258: insights into structure–DNA affinity relationships assessed by fluorescence titration measurements

Clare E. Bostock-Smith and Mark S. Searle*

Department of Chemistry, University of Nottingham, University Park, Nottingham NG7 2RD, UK

Received December 31, 1998; Revised and Accepted February 11, 1999

ABSTRACT

Fluorescence titration measurements have been used to examine the binding interaction of a number of analogues of the *bis*-benzimidazole DNA minor groove binding agent Hoechst 33258 with the decamer duplex d(GCAAATTTGC)$_2$. The method of continuous variation in ligand concentration (Job plot analysis) reveals a 1:1 binding stoichiometry for all four analogues; binding constants are independent of drug concentration (in the range [ligand] = 0.1–5 μM). The four analogues studied were chosen in order to gain some insight into the relative importance of a number of key structural features for minor groove recognition, namely (i) steric bulk of the *N*-methylpiperazine ring, (ii) ligand hydrophobicity, (iii) isohelicity with the DNA minor groove and (iv) net ligand charge. This was achieved, first, by replacing the bulky, non-planar *N*-methylpiperazine ring with a less bulky planar charged imidazole ring permitting binding to a narrower groove, secondly, by linking the *N*-methylpiperazine ring to the phenyl end of the molecule to give the molecule a more linear, less isohelical conformation and, finally, by introducing a charged imidazole ring in place of the phenolic OH making it dicationic, enabling the contribution of the additional electrostatic interaction and extended conformation to be assessed. Δ*G* values were measured at 20°C in the range –47.6 to –37.5 kJ mol^{-1} and at a number of pH values between 5.0 and 7.2. We find a very poor correlation between Δ*G* values determined by fluorescence titration and effects of ligand binding on DNA melting temperatures, concluding that isothermal titration methods provide the most reliable method of determining binding affinities. Our results indicate that the bulky *N*-methylpiperazine ring imparts a large favourable binding interaction, despite its apparent requirement for a wider minor groove, which others have suggested arises in a large part from the hydrophobic effect. The binding constant appears to be insensitive to the isohelical arrangement of the constituent rings which in these analogues gives the same register of hydrogen bonding interactions with the floor of the groove.

INTRODUCTION

The relative importance of the various contributing factors to DNA minor groove recognition by A-T selective ligands is still a matter of conjecture (1,2), despite an ever growing body of high resolution structural and thermodynamic data (3–6) from a variety of systems. A fundamental understanding of the nature of the interactions involved is desirable, not least because of the importance of these principles in the design of new compounds with altered selectivities. The *bis*-benzimidazole family of ligands provides a convenient vehicle for such investigations because of their synthetic accessibility and high binding affinities (7). Their spectroscopic characteristics have brought them into wide use as DNA fluorophores (8–12), but several have also shown potent activity against a number of microorganisms that lead to AIDS-related opportunistic infections (13–15), as well as exhibiting cytotoxic activity (16,17).

Crystallographic data on DNA complexes of Hoechst 33258 (**1**) (Fig. 1) have suggested that the sterically bulky, non-planar *N*-methylpiperazine ring exerts a primitive degree of G-C selectivity by preferring to bind in the wider minor groove associated with G-C base pairs at the end of a narrower A-T tract (18,19). The structure of the complex of an analogue in which the *N*-methylpiperazine ring has been replaced by a smaller, flatter 4,5-dihydro-3*H*-imidazol-1-ium (imidazoline) ring results in a narrower minor groove than observed for the Hoechst 33258 complex that reflects the decrease in steric bulk (20,21). Although the more planar imidazoline ring can be accommodated within the narrow A-T minor groove it does not possess the correct geometry to hydrogen bond to the groove floor. Despite this, the melting temperature of the complex is raised above that of the complex with Hoechst 33258, with the X-ray data indicating that better van der Waals complementarity with the narrow A-T minor groove, rather than hydrogen bonding, imparts the extra stability (20,21). To examine this phenomenon further, we have replaced the hydrophobic *N*-methylpiperazine ring of **1**

*To whom correspondence should be addressed. Tel: +44 115 951 3567; Fax: +44 115 951 3564; Email: mark.searle@nottingham.ac.uk

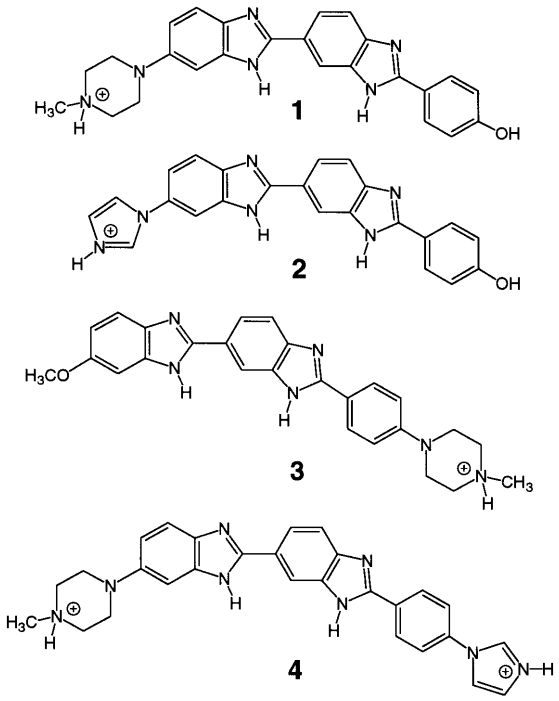

Figure 1. Chemical structures of Hoechst analogues **1–4**.

with the planar charged imidazole ring of **2** to measure the effect of a further reduction in steric bulk on groove complementarity and van der Waals interactions.

The phenomenon of isohelicity has also been examined in a number of systems and even quantitated in terms of ligand radius of curvature (22–24) and the phasing of ligand hydrogen bonding groups with the floor of the groove (25,26). A recent study of a *tris*-benzimidazole system bound to an A_3T_3 tract of DNA shows the ligand to be highly twisted to maintain hydrogen bonding complementarity with the floor of the groove, which is helped by the DNA unwinding slightly across the A tract (26). These authors conclude that ligand isohelicity, which provides a measure of van der Waals complementarity, is less important in this context than phasing of the ligand subunits with the edges of the base pairs. To address this question within the framework of a *bis*-benzimidazole binding agent, we describe an analogue (**3**) in which the *N*-methylpiperazine ring is linked to the phenyl end of the molecule rather than to the benzimidazole ring giving the molecule a more linear arrangement of the various constituent parts. The overall shape of the ligand is less isohelical with the curvature of the minor groove, although the phasing of ligand hydrogen bonding groups with the floor of the groove is identical to **1**.

Previous studies have examined the effects of ligand charge on DNA binding affinity from measurements of increases in DNA melting temperature (7,20). These results indicate that adding a second charged group to both *mono*-benzimidazole and *bis*-benzimidazole ligands increases ΔT_m by ~10°C and that this increase in ΔT_m seems to be independent of the nature of the charged group (20). Here we have characterised compound **4**, which has an imidazole ring in place of the phenolic OH of **1** making it dicationic at pH < 7, enabling the contribution of the additional electrostatic interaction and extended conformation to be assessed.

To gain insight into the relative importance of the key structural features highlighted above, all of which have been described as major factors in minor groove recognition (1,2,27), we have used equilibrium fluorescence titration measurements to estimate binding free energies for Hoechst 33258 (**1**) with the decamer duplex d(GCAAATTTGC)$_2$ and make comparisons with data for the three closely related analogues (**2**–**4**) described above (Fig. 1). This model duplex contains the A_3T_3 tract used previously in thermodynamic studies of binding of **1** (27) and in X-ray structural analysis (28,29). Within this series of Hoechst analogues we examine four key structural features: (i) steric bulk of the *N*-methylpiperazine ring; (ii) ligand hydrophobicity; (iii) isohelicity with the minor groove of DNA; (iv) net ligand charge. The data provide a foundation for understanding structure–DNA affinity relationships within this family of minor groove binding ligands.

MATERIALS AND METHODS

Materials

The DNA decamer d(GCAAATTTGC) was synthesised as previously described using standard solid phase phosphoramidite chemistry (30). *Bis*-benzimidazole analogues were provided by Hoechst.

Fluorescence spectroscopy

Fluorescence spectra were recorded on a Perkin Elmer Luminescence spectrometer LS 50 B at a temperature of 20°C in 1 cm path length polymethacrylate cuvettes. All solutions were freshly prepared as needed. Binding stoichiometries were measured by continuous variation binding analysis by the method according to Job (31,32). Both [drug] and [DNA] were varied for a fixed and constant summed concentration of 0.9 μM. Different volumes of equimolar stock solutions were mixed and made up to 3 ml with the appropriate volumes of stock buffer and H_2O to give mole fractions of drug ranging from 0.05 to 1, in 100 mM NaCl, 10 mM NaH_2PO_4 buffer. Excitation wavelengths varied from 330 to 360 nm and emission wavelengths from 390 to 420 nm according to the ligand. As some analogues fluoresce more strongly than others, slit widths were varied between 2.5 and 5 nm. Ligand binding constants were determined by equilibrium binding analysis. Fluorescence titrations were performed at a fixed concentration of ligand and the duplex concentration varied. NMR studies of a 2 mM solution of the oligonucleotide under similar conditions confirmed that the duplex was fully annealed. Aliquots of this solution were subsequently diluted for fluorescence binding studies. Ligand concentrations ranged from 0.1 to 5 μM depending both on the binding constant and the fluorescence of the drug such that $1/K_b$ was of the same order as [ligand] in order to obtain a well-defined binding isotherm. The mixture of titrant and drug was stirred for 1 min between each addition. Binding constants were determined from experimental data by fitting the following equation using a non-linear least squares procedure (Kaleidagraph software; Synergy Inc.):

$$[L_t]v^2-([L_t] + [D_t] + 1/K_{b)}v + [D_t] = 0$$

where K_b is the binding constant, $[L_t]$ is the total ligand concentration, $[D_t]$ is the total DNA concentration and v is the

fraction of drug bound, which is proportional to the measured fluorescence.

Determination of melting temperature

Optical thermal denaturation experiments were performed on a Pharmacia Biotech Ultraspec 2000 UV/Vis spectrophotometer in stoppered quartz cuvettes by using a temperature control unit connected to the spectrophotometer and a programmable heated cell holder capable of maintaining the temperature to within ±0.1°C over a range from 20 to 100°C. Melting curves for DNA and DNA–ligand complexes (3 µM) were determined by heating at 0.5°C/min until denaturation was complete, as judged from the increase in optical absorbance at 260 nm. Thermal denaturation temperatures (T_m) were determined from the maximum of the first derivative of the curve.

NMR analysis

NMR data were collected at 500 MHz on a Bruker DRX500 spectrometer using standard phase-sensitive 2D NMR pulse sequences (NOESY, DQF-COSY, TOCSY and jump-and-return NOESY for solvent suppression in 90% H_2O solutions). NMR data were collected on a 2 mM solution of duplex in 100 mM sodium chloride, 10 mM sodium phosphate buffer at pH 7.0 and 298 K.

RESULTS AND DISCUSSION

Isothermal fluorescence titration measurements

Ligand binding constants were determined in duplicate by fluorescence titration with the decamer duplex d(GCAAATTTGC)$_2$ at 20°C. All K_b values were determined at a number of [ligand], typically 0.1 and 1 µM, and were found to be independent of ligand concentration in this range. Fractional binding saturation curves are shown in Figure 2 for each of the ligands studied. Non-linear least squares analysis gives a binding constant for **1** of 3.6 (± 1.0) × 10^8 M^{-1}, indicating tight binding, in good agreement with previous estimates using A_3T_3- and A_2T_2-containing synthetic duplexes (8,27). Binding constants were determined at a number of different pH values to ensure that the imidazole ring of the unbound ligands **2** and **4** is protonated (pK_a of free imidazole ~6.5). All binding constant data are presented in Table 1. The method of continuous variation in ligand concentration was used to obtain Job plots for all ligands at a fixed value of ([ligand] + [duplex]) of 0.9 µM (31,32), giving an intersection for the fitted lines at a value close to 0.5, indicating a binding stoichiometry of drug:duplex of 1:1 in all cases (Fig. 3). While continuous variation analysis has previously shown multiple or degenerate binding stoichiometries for Hoechst 33258 with poly(dA-dT)$_2$, poly(dG-dC)$_2$] and calf-thymus DNA, these data, and those previously collected with defined sequence oligonucleotides, reveal a single high affinity drug binding site (8,27).

Differences in ligand binding energies

Ligand binding free energies determined at 20°C are presented in Table 1, together with ΔΔG values with respect to **1** at the same pH, and permit some analysis of structure–DNA affinity relationships. The results reveal unexpected differences in ligand binding energies. Substitution of the *N*-methylpiperazine with imidazole (**1**→**2**) results in a significant reduction in ligand binding energy

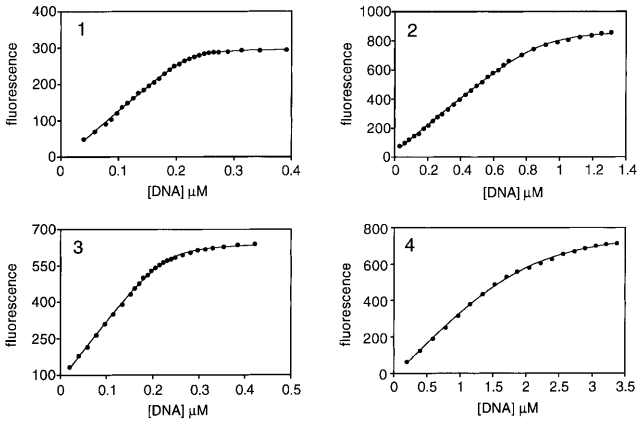

Figure 2. Fluorescence titration data for *bis*-benzimidazoles **1–4** at pH 7.2, 100 mM NaCl and 10 mM phosphate buffer. The [ligand] used was: **1**, 0.22 µM; **2**, 0.88 µM; **3**, 0.22 µM; **4**, 2.0 µM. The [DNA] was increased as shown. Fits to the data were carried out using non-linear least squares analysis as described in Materials and Methods.

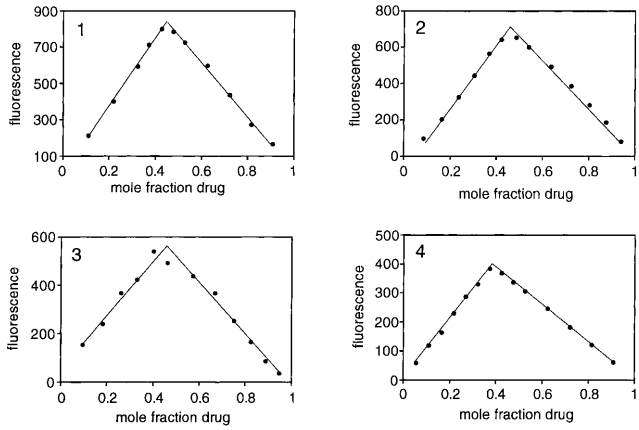

Figure 3. Job plots for *bis*-benzimidazoles **1–4** at pH 7.2. The sum of the concentrations of the ligand and DNA was kept constant at [ligand] + [DNA] = 0.9 µM. Fluorescence measurements were made at excitation wavelengths between 330 and 360 nm and emission wavelengths from 390 to 420 nm according to the ligand. The crossover points lie between 0.4 and 0.5 consistent with a drug:duplex ratio of 1:1 and reflect errors in [ligand] and [duplex] of ~15%.

of 4.7 kJ mol^{-1} at pH 7.2. A positive charge is generally regarded as a prerequisite for minor groove binding so we also measured the binding affinities at pH 5.0 to ensure that the unbound imidazole ring is fully protonated. The binding of Hoechst 33258 (**1**) is insensitive to pH over this range (Table 1), however, K_b for **2** decreased by a small amount ($\Delta\Delta G_{\mathbf{1}\rightarrow\mathbf{2}}$ ~ 7.5 kJ mol^{-1}, pH 5.0). These data indicate that the less bulky imidazole ring, which presumably can be accommodated within a narrower minor groove, does not lead to a better binding interaction in this context. Despite the greater steric bulk and the requirement for a wider minor groove, the *N*-methylpiperazine ring appears to impart a more favourable binding interaction. The hydrophobic contribution to binding has recently been emphasised by detailed calorimetric studies of Hoechst 33258 with an analoguous A_3T_3 duplex (27). A large change in heat capacity on binding and an entropy-driven interaction strongly suggests that the hydrophobic effect contributes

the major component of the binding energy. Although in the X-ray structures the *N*-methylpiperazine ring of Hoechst 33258 makes relatively poor van der Waals interactions (28) compared with the imidazoline analogue (20,21), the burial of hydrophobic surface area in the former is larger. Our thermodynamic analysis similarly suggests that the imidazole ring of **2** will probably bind to a narrow minor groove but the van der Waals contacts formed are not as beneficial to binding as the hydrophobic interaction of the *N*-methylpiperazine ring.

Table 1. Flourescence binding data and ΔT_m values ($T_m^{complex} - T_m^{free\ duplex}$) for Hoechst analogues binding to d(GCAAATTTGC)$_2$

Compound	K_b (M^{-1})	ΔG (kJ mol^{-1})	$\Delta\Delta G$ (kJ mol^{-1})[a]	ΔT_m (K)[b]
1	$3.6 (\pm 1.0) \times 10^8$	–47.3	–	15.5
	$3.1 (\pm 1.0) \times 10^8$ [c]	–47.0[c]	–	23.2[c]
2	$5.0 (\pm 2.0) \times 10^7$	–42.6	4.7	17.6
	$1.4 (\pm 1.0) \times 10^7$ [c]	–39.5[c]	7.5[c]	27.2
3	$4.2 (\pm 2.0) \times 10^8$	–47.6	–0.3	15.3
				24.2[c]
4	$6.0 (\pm 2.0) \times 10^6$	–37.5	9.8	20.1
	$1.3 (\pm 2.0) \times 10^7$ [d]	–39.4[d]	–	–
	$1.4 (\pm 2.0) \times 10^7$ [c]	–39.5[c]	7.5[c]	26.3[c]

[a]$\Delta\Delta G$ values with respect to compound **1**.
[b]$T_m^{free\ duplex}$ = 39.1°C.
All data at pH 7.2, 20°C unless indicated. [c]Data at pH 5.0; [d]data at pH 6.0.

Examining the importance of isohelicity (**1** versus **3**) reveals that the more linear analogue binds to the A-T minor groove with an affinity indistinguishable from **1**, $\Delta\Delta G \sim -0.3$ kJ mol^{-1}. Thus, in this context, the subtle difference in curvature between **1** and **3** appears to have little effect on DNA binding affinity. Both Hoechst 33258 and **3** are able to adopt the same phasing of hydrogen bonding interactions with the floor of the minor groove since the benzimidazole NH groups in both ligands have identical spacing. It is, however, evident from model building studies that the *N*-methylpiperazine ring of **3** does not lie as deeply in the groove as is observed in the X-ray structures of Hoechst 33258 (28,29). This does not preclude the possibility that the conformation of the DNA minor groove adjusts to accommodate the bound ligand. Clark *et al.* (26) have already illustrated this 'induced-fit' interaction in their study of a *tris*-benzimidazole analogue which does not show optimal isohelicity with the minor groove but induces a slight unwinding (reduction in twist) of the helix within the A_3T_3 tract.

Finally, we examined the dicationic analogue **4**. At pH 7.2 we found that **4** also bound significantly less tightly than **1** ($\Delta\Delta G \sim$ 9.8 kJ mol^{-1}, pH 7.2), with a small increase in affinity of **4** at lower pH (Table 1). This latter observation was surprising in the light of previous observations that dicationic ligands result in increases in ΔT_m values of ~10°C over their monocationic counterparts. To draw conclusions regarding the relationship between ΔG values measured under isothermal conditions and those derived from T_m measurements we have determined the latter at similar concentrations to those used in fluorescence experiments and at several different pH values (Table 1).

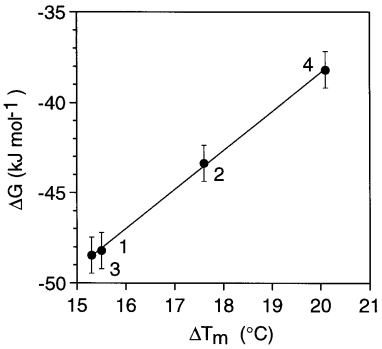

Figure 4. Correlation plot of ΔG for the binding of *bis*-benzimidazoles **1–4** to d(GCAAATTTGC)$_2$ at pH 7.2 determined by fluorescence titration at 20°C, versus ΔT_m values determined at [DNA] = 3 μM, in 100 mM NaCl and 10 mM phosphate buffer.

Equilibrium binding constants versus UV melting data

Previous studies (7,23) have used differences in DNA melting temperatures between free duplex and ligand-bound duplex (ΔT_m) to estimate binding constants (K_b) based on an implicit correlation between the two that assumes similarities in thermodynamic parameters for binding. For the purpose of direct comparison with the isothermal fluorescence titration measurements described above, we have also determined ΔT_m values from UV melting curves in the same buffer and at duplex concentrations of 3 μM at pH 7.2 and 5.0. Surprisingly, we find an inverse correlation between ΔT_m and ΔG (Fig. 4). Although ΔT_m and ΔG are similar for **1** and **3**, a higher ΔT_m value for **2** contrasts with a smaller binding constant than for **1** by a factor of ~8. The trend is further evident with the dicationic ligand **4**, which has the smallest binding energy but the highest ΔT_m. The data highlight the complexity of using ΔT_m values to assess binding affinities when the temperature dependence of binding constants has not been first characterised. The detailed calorimetric analysis of the binding of Hoechst 33258 to a similar A_3T_3 dodecamer duplex, as described above, has revealed a large negative ΔC_p° that accompanies binding (27), consistent with the hydrophobic effect contributing significantly to the binding free energy. Such a large ΔC_p° term makes measurement of binding constants highly temperature dependent such that structural changes to a ligand (**1**→**2**) that modify the hydrophobic surface area buried on binding (and hence ΔC_p°) are likely to have a significant impact on ΔT_m values. Thus, measurements of binding constants attained under isothermal conditions appear to be the most reliable method of drawing conclusions regarding structure–binding relationships.

NMR footprinting analysis

The above analysis assumes that the ligands described are binding at a similar site within the minor groove of the A_3T_3 tract. To support this assumption we have carried out an NMR structural analysis of the 1:1 complex of **3** with the same decamer duplex d(GCAAATTTGC)$_2$ to establish whether there are any gross differences in the mode of binding of **1** and **3** that fortuitously result in similar binding affinities. To examine more closely the location of the drug within the groove we have used perturbations to ^{1}H chemical shifts ($\Delta\delta = \delta_{bound} - \delta_{free}$) to provide an NMR 'footprint' (33). $\Delta\delta$ values for deoxyribose H1′ and base H6/H8

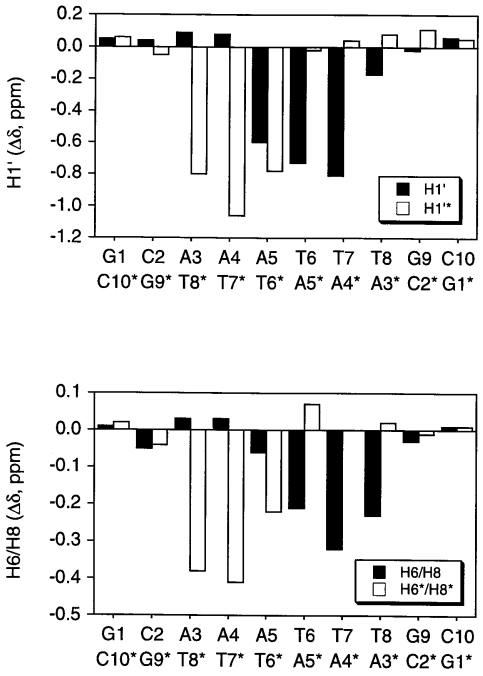

Figure 5. Plots of drug-induced changes in ^{1}H chemical shifts (Δδ) for deoxyribose H1′ (top) and base H6/H8 (bottom) for the complex of **3** bound to d(GCAAATTTGC)$_2$. Data collected at 500 MHz at 298 K. The two strands of DNA read in anti-parallel directions, one of which is distinguished by the use of asterisks and unfilled columns.

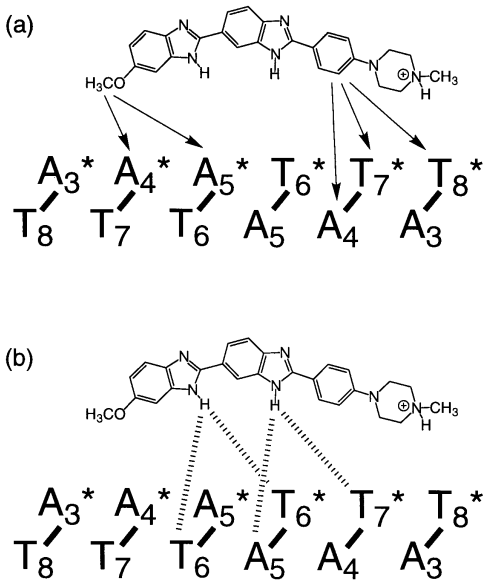

Figure 6. (**a**) Schematic representation of the 1:1 complex of **3** bound to d(GCAAATTTGC)$_2$ highlighting a few key intermolecular NOEs. (**b**) Dashed lines represent bifurcated hydrogen bonds from the benzimidazole NH groups to thymine O2 or adenine N3 in the minor groove derived from modelling studies. The two strands of the duplex are distinguished by the use of an asterisk.

resonances are plotted against sequence position in Figure 5. Many of the deoxyribose H1′ groups, which are located on the walls of the minor groove, come into direct contact with the face of one or other aromatic ring of the bound ligand and many undergo large ring current perturbations to their chemical shifts (–0.6 and –1.1 p.p.m.) (34) and are, therefore, particularly sensitive to the position of the ligand within the minor groove. Large Δδ values are particularly evident for the thymine sugars while perturbations to the resonances of the flanking G-C base pairs are small by comparison (<0.1 p.p.m.), clearly identifying the bound ligand within the A_3T_3 tract. Although Δδ H6/H8 values are smaller, the pattern of perturbations reflects that observed for the deoxyribose H1′. Notably, both sets of resonances suggest a relatively centro-symmetric orientation of the *bis*-benzimidazole portion of the ligand across the dyad axis. NOEs from the benzimidazole methoxy group to the deoxyribose H1′ and base H2 of A4* and A5* and from the phenyl ring protons to deoxyribose H1′ of A4, T7* and T8* have enabled the orientation of **3** in the minor groove to be established unambiguously, locating the *N*-methylpiperazine ring close to the end of the A-T tract (Fig. 6). Our initial model of the complex of **3** shows the binding locus for the two benzimidazole rings to be similar to that seen for the A_3T_3 complex of **1** in the X-ray structure of Vega *et al.* (29), leading us to suggest a similar pattern of bifurcated hydrogen bonds to the floor of the minor groove (Fig. 6). Despite the more linear structure of **3** and our initial perception of poorer isohelical complementarity with the curvature of the minor groove, fluorescence binding data and NMR analysis have established a high binding affinity compatible with its location at the centre of the minor groove of the A-T tract. Consistent with the model of Clark *et al.* (26), isohelicity need not be optimal provided the register of hydrogen bonds with the floor of the groove is maintained. Hydrophobic surface burial may still be an important contributing factor in the binding of the *N*-methylpiperazine ring despite the fact that it does not appear to lie as deeply within the minor groove.

A full description of the drug recognition process is clearly dependent on detailed structural and energetic analysis if a cohesive, robust understanding of molecular interactions is to develop. Structural analysis of the complexes described is currently underway, together with investigations of other A tract sequences.

ACKNOWLEDGEMENTS

We thank John Keyte (School of Biomedical Sciences) for oligonucleotide synthesis, Dr Neil Thomas for access to a fluorescence spectrophotometer and Professor Terry Jenkins for helpful comments on the manuscript. We are grateful to the Department of Chemistry and the University of Nottingham for financial contributions to this work and to Hoechst, Germany, for providing the compounds described. C.E.B.-S. is grateful to the EPSRC for a research studentship.

REFERENCES

1 Clark,G.R., Squire,C.J., Gray,E.J., Leupin,W. and Neidle,S. (1996) *Nucleic Acids Res.*, **24**, 4882–4886.
2 Clark,G.R., Boykin,D.W., Czarny,A. and Neidle,S. (1997) *Nucleic Acids Res.*, **25**, 1510–1515.
3 Marky,L.A. and Breslauer,K.J. (1987) *Proc. Natl Acad. Sci. USA*, **84**, 4359–4363.
4 Misra,V.K., Sharp,K.A., Friedman,R.A. and Honig,B. (1994) *J. Mol. Biol.*, **238**, 245–263.
5 Rentzeperis,D. and Marky,L.A. (1993) *J. Am. Chem. Soc.*, **115**, 1645–1650.
6 Schmitz,H.-U. and Hubner,W. (1993) *Biophys. Chem.*, **48**, 61–74.

7 Lombardy,R.L., Tanious,F.A., Ramachandran,K., Tidwell,R.R. and Wilson,W.D. (1996) *J. Med. Chem*., **39**, 1452–1462.
8 Loontiens,F.G., McLaughlin,L.W., Diekmann,S. and Clegg,R.M. (1991) *Biochemistry*, **30**, 182–189.
9 Ellwart,J.W. and Dormer,P. (1990) *Cytometry*, **11**, 239–243.
10 Stokke,T. and Steen,H.B. (1985) *J. Histochem. Cytochem*., **33**, 333–338.
11 Latt,S.A. and Wohleb,J.C. (1975) *Chromosoma*, **52**, 297–316.
12 Bailly,C., Colson,P., Henichart,J.P. and Houssier,C. (1993) *Nucleic Acids Res*., **21**, 3705–3711.
13 Bell,C.A., Dykstra,C.C., Naiman,N.A., Cory,M., Fairley,T.A. and Tidwell,R.R. (1993) *Antimicrob. Agents Chemother.*, **37**, 2668–2673.
14 Tidwell,R.R., Jones,S.K.,Naiman,N.A., Berger,L.C., Brake,W.B., Dykstra,C.C. and Hall,J.E. (1993) *Antimicrob. Agents Chemother.*, **37**, 1713–1716.
15 Fairley,T.A., Tidwell,R.R., Donkor,I., Naiman,N.A., Ohemeng,K.A., Lombardy,R., Bentley,J.A. and Cory,M. (1993) *J. Med. Chem*., **36**, 1746–1753.
16 Chen,A.Y., Chiang,Y., Gatto,B. and Lui,L.F. (1993) *Proc. Natl Acad. Sci. USA*, **90**, 8131–8135.
17 Patel,S.R., Kvols,L.K., Rubin,J., O'Connell,M.J., Edmonson,J.H., Ames,M.M. and Kovach,J.S. (1991) *Invest. New Drugs*, **9**, 53–57.
18 Pjura,P.E., Grzeskowiak,K. and Dickerson,R.E. (1987) *J. Mol. Biol*., **197**, 257–271.
19 Carrondo,M.A.A.F. de C.T., Coll,M., Aymami,J., Wang,A.H.-J., van der Marel,G.A., van Boom,J.H. and Rich,A. (1989) *Biochemistry*, **28**, 7849–7859.
20 Czarny,A., Boykin,D.W., Wood,A.A, Nunn,C.M., Neidle,S., Zhao,M. and Wilson,W.D. (1995) *J. Am. Chem. Soc*., **117**, 4716–4717.
21 Wood,A.A., Nunn.,C.M., Czarny,A., Boykin,D.W. and Neidle,S. (1995) *Nucleic Acids Res*., **23**, 3678–3684.
22 Goodsell,D. and Dickerson,R.E. (1986) *J. Med. Chem*., **29**, 727–733.
23 Zasedatelev,A.S. (1991) *FEBS Lett*., **28**, 209–211.
24 Cory,M.J., Tidwell,R.J. and Fairley,T.A. (1992) *J. Med. Chem*., **25**, 431–438.
25 Youngquist,R.S. and Dervan,P.B. (1985) *Proc. Natl Acad. Sci. USA*, **82**, 2565–2569.
26 Clark,G.R., Gray,E.J., Neidle,S., Li.,Y.-H. and Leupin,W. (1996) *Biochemistry*, **35**, 13745–13752.
27 Haq,I., Ladbury,J.E., Chowdhry,B.Z., Jenkins,T.C. and Chaires,J.B. (1997) *J. Mol. Biol*., **271**, 244–257.
28 Spink,N., Brown,D.G., Skelly,J.V. and Neidle,S. (1994) *Nucleic Acids Res*., **22**, 1607–1612.
29 Vega,M.C., Garcia-Saez, Aymami,J., Eritja,T., van der Marel,G.A., van Boom,J.H., Rich,A. and Coll,M. (1994) *Eur. J. Biochem*., **222**, 721–726.
30 Bostock-Smith,C.E., Laughton,C.A. and Searle,M.S. (1998) *Nucleic Acids Res*., **26**, 1660–1667.
31 Job,P. (1928) *Ann. Chim. (Paris)*, **9**, 113–203.
32 Lohman,T.M. and Mascotti,D.P. (1992) *Mehods Enzymol*., **212**, 424–458.
33 Embrey,K.J., Searle,M.S. and Craik,D.J. (1991) *J. Chem. Soc. Chem. Commun*., 1770–1771.
34 Embrey,K.J., Searle,M.S. and Craik,D.J. (1993) *Eur. J. Biochem*., **211**, 437–447.